Immunity
Article

Galectin-1 Deactivates Classically Activated Microglia and Protects from Inflammation-Induced Neurodegeneration

Sarah C. Starossom,[1,7] Ivan D. Mascanfroni,[2,7] Jaime Imitola,[1] Li Cao,[1,3] Khadir Raddassi,[1] Silvia F. Hernandez,[2] Ribal Bassil,[1] Diego O. Croci,[2] Juan P. Cerliani,[2] Delphine Delacour,[4] Yue Wang,[1] Wassim Elyaman,[1] Samia J. Khoury,[1,5,8,*] and Gabriel A. Rabinovich[2,6,8,*]

[1]Center for Neurologic Diseases, Brigham and Women's Hospital, Harvard Medical School, Boston, MA 02115, USA
[2]Laboratorio de Inmunopatología, Instituto de Biología y Medicina Experimental (IBYME), Consejo Nacional de Investigaciones Científicas y Técnicas (CONICET), Buenos Aires 1428, Argentina
[3]Department of Neurobiology, Institute of Neurosciences, Second Military Medical University, Shanghai 200433, China
[4]Department of Developmental Biology, Institut Jacques Monod, CNRS 7592, Paris-Diderot University, 75205 Paris, France
[5]Abu Haidar Neuroscience Institute, American University of Beirut, Beirut 1107 2020, Lebanon
[6]Laboratorio de Glicómica Funcional, Departamento de Química Biológica, Facultad de Ciencias Exactas y Naturales, Universidad de Buenos Aires, Buenos Aires 1428, Argentina
[7]These authors contributed equally to this work
[8]These authors contributed equally to this work
*Correspondence: skhoury@rics.bwh.harvard.edu (S.J.K.), gabyrabi@gmail.com (G.A.R.)
http://dx.doi.org/10.1016/j.immuni.2012.05.023

SUMMARY

Inflammation-mediated neurodegeneration occurs in the acute and the chronic phases of multiple sclerosis (MS) and its animal model, experimental autoimmune encephalomyelitis (EAE). Classically activated (M1) microglia are key players mediating this process. Here, we identified Galectin-1 (Gal1), an endogenous glycan-binding protein, as a pivotal regulator of M1 microglial activation that targets the activation of p38MAPK-, CREB-, and NF-κB-dependent signaling pathways and hierarchically suppresses downstream proinflammatory mediators, such as iNOS, TNF, and CCL2. Gal1 bound to core 2 O-glycans on CD45, favoring retention of this glycoprotein on the microglial cell surface and augmenting its phosphatase activity and inhibitory function. Gal1 was highly expressed in the acute phase of EAE, and its targeted deletion resulted in pronounced inflammation-induced neurodegeneration. Adoptive transfer of Gal1-secreting astrocytes or administration of recombinant Gal1 suppressed EAE through mechanisms involving microglial deactivation. Thus, Gal1-glycan interactions are essential in tempering microglial activation, brain inflammation, and neurodegeneration, with critical therapeutic implications for MS.

INTRODUCTION

Multiple sclerosis (MS) is a chronic inflammatory demyelinating and degenerative disease of the CNS. The clinical disease course usually starts with reversible episodes of neurological disability (relapsing-remitting MS, or RRMS), which later develops into a progressive stage with irreversible neurological decline (secondary progressive MS, or SPMS) (Trapp and Nave, 2008). Axonal loss occurs in both the acute and chronic phases of MS and its animal model, experimental autoimmune encephalomyelitis (EAE), and the loss of compensatory CNS mechanisms contributes to the transition from RRMS to SPMS (Zamvil and Steinman, 2003).

Activated microglia and macrophages are thought to contribute to neurodegeneration, as their number correlates with the extent of axonal damage in MS lesions (Bitsch et al., 2000; Rasmussen et al., 2007) and with neuronal dysfunction in EAE (Weiner, 2009). Microglia and macrophages can be activated by the cytokines interferon-γ (IFN-γ), interleukin-17 (IL-17), or lipopolysaccharide (LPS) into a proinflammatory phenotype (M1), whereas IL-4 or IL-13 induce a state of alternative activation (M2), which is associated with neuroprotective functions that promote repair (Ponomarev et al., 2007; Butovsky et al., 2006; Kawanokuchi et al., 2008).

Recent efforts toward decoding the information encoded by the glycome revealed essential roles of glycan-binding proteins or lectins in the regulation of immune tolerance and inflammation (Rabinovich and Croci, 2012). Galectins, a family of endogenous lectins, function in the extracellular milieu by interacting with a myriad of glycosylated receptors on the surface of immune cells (Rabinovich and Croci, 2012). However, these lectins may also play roles inside the cells, including modulation of intracellular signaling pathways. Although originally defined by their ability to recognize the disaccharide N-acetyllactosamine [Galβ(1–4)-GlcNAc; LacNAc], recent evidence indicates substantial differences in the glycan-binding preferences of individual members of the galectin family (Rabinovich and Croci, 2012). Galectin-1 (Gal1; encoded by *Lgals1*) has been implicated in the regulation of innate and adaptive immunity. In the periphery, Gal1 promotes selective apoptosis of T helper (Th) 1 and Th17 cells (Toscano et al., 2007), induces IL-10 secretion

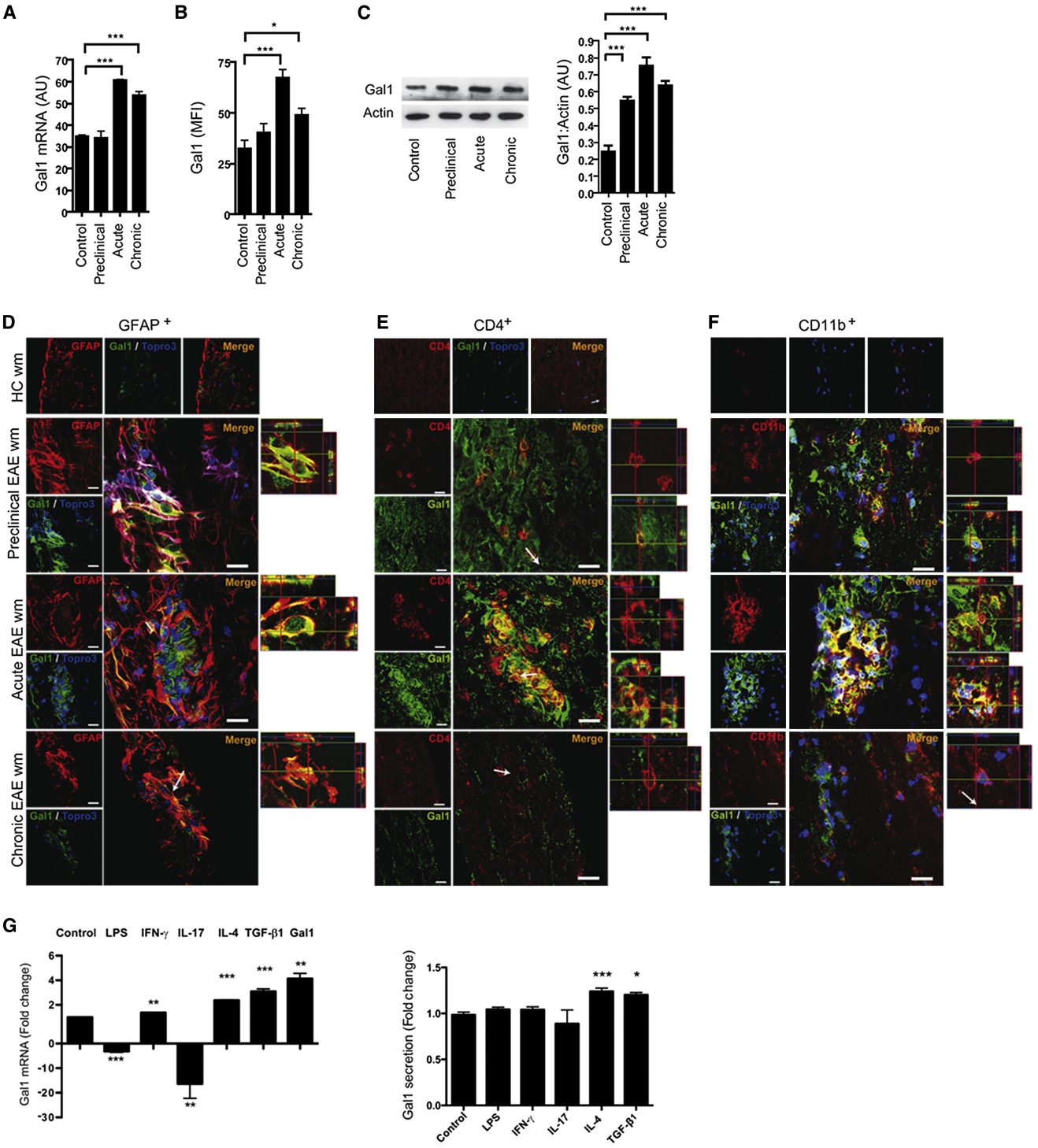

Figure 1. CNS Expression of Gal1 Is Dynamically Regulated during EAE

(A–F) Gal1 mRNA and protein expression in mouse spinal cord tissue and confocal microscopy of spinal cord white matter sections from CFA-immunized (control), preclinical EAE (preclinical, 10 dpi), acute EAE (acute, 20 dpi), and chronic EAE (chronic, 40 dpi) mice.

(A) Relative Gal1 mRNA expression in mouse spinal cord tissue.

(B) Mean fluorescence intensity (MFI) of Gal1 immunoreactivity in mouse spinal cord white matter (wm).

(C) Immunoblot of Gal1 expression in mouse spinal cord tissue.

(D–F) Confocal microscopy analysis. Sections were stained with Gal1 antibody (green), the nuclear marker Topro3 (blue) and GFAP (D, red), CD4 (E, red), or CD11b (F, red) antibodies. Scale bars represent 20 μm (left panel). Right panels show three-dimensional (3D) reconstruction ortho-view micrographs of representative cells. The images of every marker were acquired using the same parameters.

(van der Leij et al., 2007; Stowell et al., 2008; Cedeno-Laurent et al., 2012), inhibits T cell trafficking (Norling et al., 2008), and decreases antigen-presenting capacity and nitric oxide (NO) production by macrophages (Barrionuevo et al., 2007; Correa et al., 2003). Furthermore, exposure to Gal1 promotes the differentiation of IL-27-producing tolerogenic dendritic cells (DCs) (Ilarregui et al., 2009) and favors the expansion of inducible regulatory T (iTreg) cells (Toscano et al., 2006); however, the function of this lectin on endogenous CNS innate immunity is unknown.

Here, we show that endogenous and exogenous Gal1 plays a pivotal role in deactivating classically activated microglia and promoting a phenotype of alternative activation through modulation of the mitogen-activated protein kinase p38 (p38MAPK), cAMP response element binding (CREB), and nuclear factor kappa-light-chain-enhancer of activated B cells (NF-κB) signaling pathways. This effect involved binding of Gal1 to core 2 O-glycans on CD45, which promoted retention of this glycoprotein on the microglial cell surface and augmented its phosphatase activity. In vivo, Gal1 prevented microglial activation and promoted neuroprotection. Our findings suggest a glycosylation-dependent mechanism for preventing inflammation-induced neurodegeneration through selective deactivation of microglial cells.

RESULTS

Dynamic Regulation of Endogenous Gal1 in CNS Cells

Gal1 expression in the spinal cord was analyzed at the mRNA level (Figure 1A) and at the protein level (Figures 1B and 1C) in the white matter of the spinal cord tissue in naive mice and in mice with MOG-induced EAE at the preclinical stage (day 10 postimmunization), at the peak of disease (day 15–16 postimmunization), and at the chronic stage (day 30–40 postimmunization). In naive mice, there was very little expression of Gal1 in the CNS, but during the preclinical phase, Gal1 protein expression was increased (Figures 1B and 1C), whereas Gal1 mRNA expression was unchanged (Figure 1A). Gal1 expression was highest at the peak of disease and persisted at lower levels during the chronic phase of EAE (Figures 1A–1C). Of note, Gal1 was highly expressed in $GFAP^+$ astrocytes bordering the lesion area (Figure 1D), in a subset of $CD4^+$ T cells (Figure 1E), and in a subset of $CD11b^+$ cells (Figure 1F) during preclinical and acute EAE. During the chronic phase of EAE, only astrocytes maintained considerable expression of this lectin (Figure 1D).

These observations prompted us to investigate the potential stimuli that induce expression of this lectin. In astrocytes, we observed strong downregulation of Gal1 mRNA following stimulation with LPS or IL-17A, a slight increase after IFN-γ treatment, and strong upregulation after exposure to anti-inflammatory stimuli, such as IL-4, transforming growth factor β1 (TGF-β1), and Gal1 itself (Figure 1G). However, only stimulation of astrocytes with IL-4 and TGF-β1 led to a significant increase in secreted Gal1 (Figure 1G).

We then analyzed Gal1 mRNA expression and Gal1 secretion in in vitro-differentiated Th1, Th2, Th17 and iTreg cells, and Gal1 mRNA expression in ex vivo-isolated natural regulatory T (nTreg) cells. Gal1 mRNA was downregulated in Th1 and Th2 cells, but not in Th17 and iTreg cells, as compared to nonpolarized activated T cells (Th0) (Figure S1A available online). Moreover, there was a trend toward a decrease in Gal1 secretion in all subsets as compared to nonpolarized T cells (Figure S1B). $FoxP3^+GFP^+$ nTreg cells that were isolated from the spleen of naive mice showed higher Gal1 mRNA expression compared to $FoxP3^-GFP^-$ cells (Figure S1C). Similarly, $FoxP3^+CD4^+$ T cells isolated from the CNS showed increased Gal1 expression compared to the $FoxP3^-$ population during preclinical and acute EAE (Figure S1D), although both populations had increased expression during acute EAE compared to preclinical EAE.

Similar to our observations in astrocytes, anti-inflammatory or Th2 cell-type stimuli led to substantial upregulation of Gal1 mRNA expression and secretion in microglia, whereas Gal1 mRNA was downregulated upon exposure to LPS or IFN-γ (Figures S1E and S1F). Exposure to IL-17A did not affect Gal1 mRNA expression or Gal1 secretion. Furthermore, Gal1 itself slightly increased Gal1 mRNA expression (Figure S1E), suggesting that Gal1 might act in an autocrine manner to control microglial responses.

Gal1 Controls M1 Microglial Activation through Modulation of p38MAPK, CREB, and NF-κB Signaling Pathways

Activation with LPS or IFN-γ induces an M1 phenotype in microglial cells that is characterized by high major histocompatibility complex class II (MHC II), CD86, and inducible nitric oxide (iNOS) expression and production of proinflammatory cytokines and chemokines, such as tumor necrosis factor (TNF) and CCL2, whereas stimulation with IL-4 induces an M2 phenotype characterized by arginase expression (Ponomarev et al., 2007). We investigated the binding of Gal1 to M1 or M2 microglia. Gal1 bound to isolated primary microglia in a dose- and saccharide-dependent fashion (Figure 2A and Figure S2). Gal1 binding was markedly increased when microglia were polarized toward an M1 phenotype (Figure 2A). In contrast, Gal1 binding to M2-polarized microglia was substantially decreased compared to unstimulated microglia (Figure 2A). To determine whether differential binding to M1- or M2-activated microglia correlates with distinct glycosylation signatures, we compared the glycophenotype of these cells using a panel of plant lectins that selectively recognize specific oligosaccharide sequences (Toscano et al., 2007). Whereas *Sambucus nigra agglutinin* (SNA) recognizes α2-6-linked sialic acid, which interferes with Gal1 binding, *Maackia amurensis* agglutinin (MAL II) binds to α2-3 sialic acid linkages, L-phytohemagglutinin (L-PHA) recognizes β1-6 branching on complex N-glycans, peanut agglutinin (PNA) recognizes asialo-galactose β1-3-N-acetylgalactosamine (core-1) O-glycans, and *Helix pomatia* (HPA) binds specifically to terminal

(G) Effect of stimulation of astrocytes with LPS (10 ng/ml), IFN-γ (10 ng/ml), IL-17A (10 ng/ml), IL-4 (10 ng/ml), TGF-β1 (5 ng/ml), and recombinant Gal1 (5 μg/ml) on Gal1 mRNA expression and secretion.

Data are representative (C–F) or are the mean ± SEM (A, B, C, and G) of three independent experiments. *$p < 0.05$; **$p < 0.01$; ***$p < 0.005$ versus control. AU, arbitrary units; HC, healthy control.

See also Figure S1.

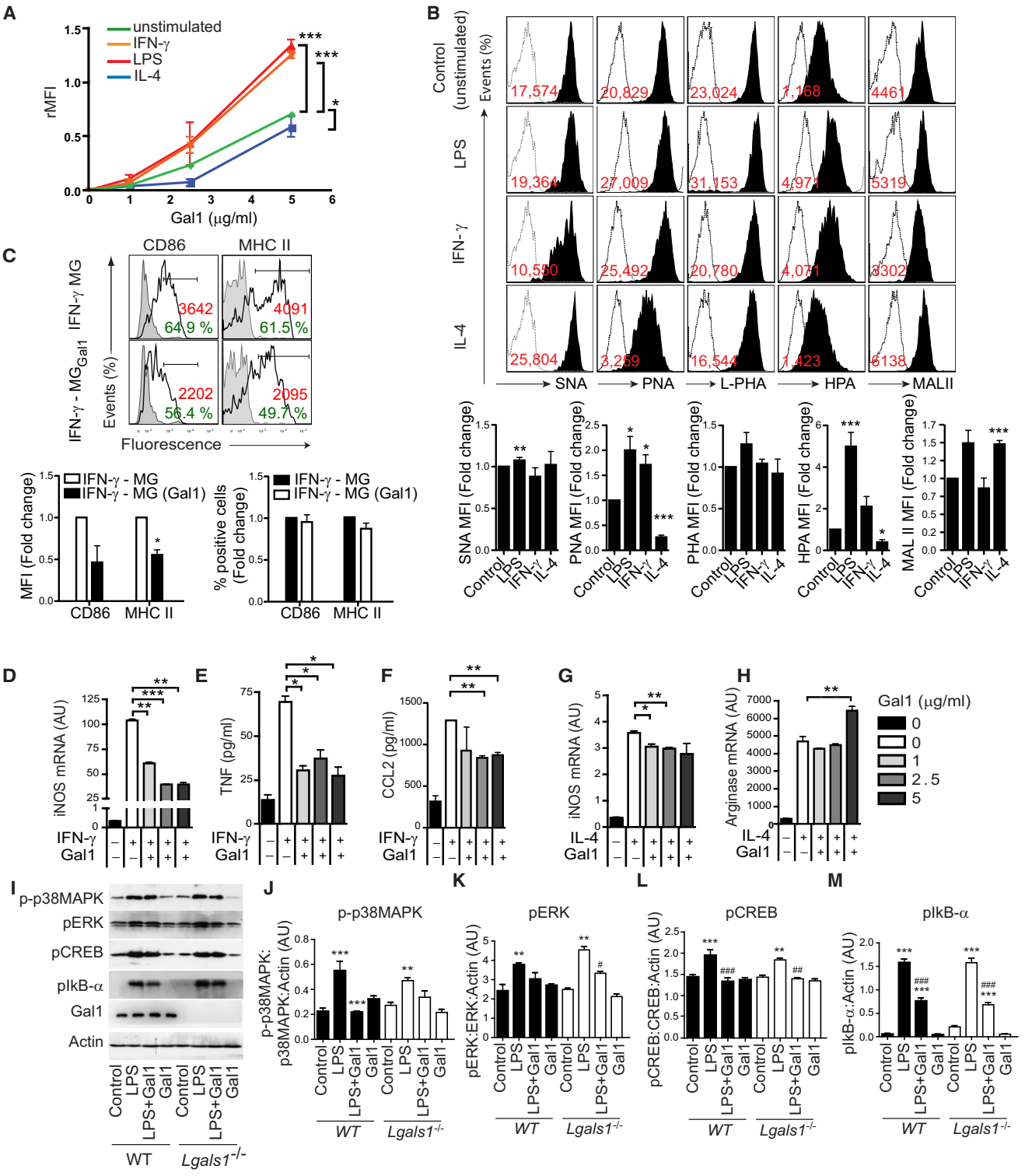

Figure 2. Gal1 Differentially Modulates Microglia Activation In Vitro

(A) Flow cytometry of resting and polarized microglial subsets incubated with increasing concentrations of recombinant Gal1.

(B) Expression of cell-surface glycans on M1 (LPS, IFN-γ), M2 (IL-4), and resting (unstimulated) microglia, detected with biotinylated SNA, PNA, L-PHA, HPA, and MAL II (black filled histograms) or with FITC-conjugated streptavidin alone (dashed open histograms). Red numbers represent the relative median of intensity (median of intensity [lectin]–median of intensity [streptavidin control]). Bar diagrams display the lectin binding as fold change relative to unstimulated microglia.

(C) Flow cytometry of M1 microglia activated by IFN-γ (24 hr). Control (IFN-γ-MG) or Gal1-treated (IFN-γ-MG_{Gal1}) microglia were stained with antibodies against CD86 and MHC II. Black lines represent specific antibody binding, whereas tinted lines represent unspecific fluorescence signal. Percentage of positive cells and

α-N-acetylgalactosamine residues (Hirabayashi et al., 2002). Notably, we found augmented unsialylated core 1 O-glycans in M1 (LPS or IFN-γ)-polarized compared to M2 (IL-4)-polarized microglia, as shown by abundant reactivity of these cells to PNA. Augmented PNA reactivity indicates increased availability of glycan structures required for elongation of core 2 O-glycans through the action of the core 2 β1,6-N-acetylglucosaminyltransferase 1 (C2GnT1), which favors LacNAc incorporation and galectin binding (Tsuboi et al., 2011). In addition, M1 microglia showed higher binding capacity to L-PHA, suggesting increased β1,6 branching of complex N-glycans (ligands for galectins) that are generated by the enzyme β1,6 N-acetylglucosaminyltransferase 5 (GnT5) (Partridge et al., 2004). This lectin-binding pattern was accompanied by higher HPA reactivity in M1 versus M2 microglia. Also, there was a trend toward higher binding of SNA to M2 microglia, consistent with the well-recognized ability of α2-6-linked sialic acid to interfere with Gal1 binding. Finally, both M1- and M2-polarized microglia had similar binding profiles for MAL II, although IFN-γ-stimulated cells had lower MAL II binding. As α2,3-linked sialic acid may allow binding of Gal1 with different affinities than asialo-LacNAc structures (Hirabayashi et al., 2002), these results suggest that subtle differences may exist in the glycoprofile of different subpopulations of classically activated (LPS or IFN-γ) microglia (Figure 2B). Collectively, these findings suggest that M1 microglia, but not M2 microglia, express the preferred set of glycans required for Gal1 binding and function.

To determine whether Gal1 binding to microglia results in phenotypic or functional changes, we first analyzed the cell surface phenotype of these cells. In IFN-γ-polarized M1 microglia, surface expression of MHC II and CD86 was substantially decreased following exposure to recombinant Gal1 (Figure 2C). Furthermore, expression of iNOS mRNA and production of TNF and CCL2 were significantly decreased by Gal1 in M1 microglia (Figures 2D–2F and S3A–S3C). In contrast, M2-polarized microglia experienced a relative increase in arginase and iNOS mRNA compared to unstimuated microglia, yet exposure to Gal1 (at its highest dose) enhanced arginase mRNA expression but decreased iNOS mRNA expression (Figures 2G and 2H). This effect was also observed in LPS-stimulated Gal1-treated microglia (Figure S3D). Although Gal1 selectively deletes Th1 and Th17 cells (Toscano et al., 2007), we could find no effect of this lectin on the viability of microglial cells at concentrations ranging from 1 to 10 μg/ml (data not shown).

The production of NO and TNF is controlled by proinflammatory signaling pathways involving NF-κB (Zhang et al., 2010), extracellular signal-regulated kinase (ERK) (Cui et al., 2010), p38MAPK (Xing et al., 2008), and CREB (Mirzoeva et al., 1999). We investigated the effect of Gal1 on the phosphorylation of these signaling molecules in primary microglial cells from wild-type (WT) and Gal1-deficient (*Lgals1*$^{-/-}$) mice. LPS induced phosphorylation of the inhibitor of κB-α (IκB-α), a negative regulator of the NF-κB pathway, after 5 min, and of p38MAPK, ERK, and CREB after 15 min of incubation (Figures 2I–2M). However, activation of microglia with LPS in the presence of Gal1 induced a significant decrease in the phosphorylation of p38, CREB, and IκB-α, but only slight inhibition in the phosphorylation of ERK (Figures 2I–2M). Thus, Gal1 acts by limiting microglial activation mainly through modulation of p38-, CREB- and NF-κB-dependent pathways. Notably, there were no significant differences in the phosphorylation pattern of WT and *Lgals1*$^{-/-}$ microglia exposed to Gal1 (Figures 2I–2M), suggesting that cell-intrinsic Gal1 does not play a substantial role in the modulatory effects of exogenous Gal1.

Gal1 Promotes Retention of CD45 on the Surface of Microglial Cells and Augments Its Phosphatase Activity

CD45 is a heavily glycosylated protein tyrosine phosphatase that negatively regulates M1 microglial activation, leading to the promotion of an M2 phenotype (Salemi et al., 2011). Because Gal1 binds to CD45 on T cells (Earl et al., 2010), we hypothesized that Gal1-glycan interactions may promote microglial deactivation by specifically retaining CD45 on the cell surface, thereby augmenting its phosphatase activity and prolonging transmission of inhibitory signals. Coimmunoprecipitation experiments with lysates of BV-2 microglial cells treated with Gal1 revealed specific interactions between Gal1 and CD45 (Figure 3A). Supporting these findings, exogenously added Gal1 colocalized with CD45 on M1 microglial cells (Figure 3B). Notably, flow-cytometric analysis of nonpermeabilized cells demonstrated time-dependent retention of CD45 on the surface of LPS-stimulated M1 microglia exposed to Gal1 compared to cells treated with vehicle control (Figure 3C). This resulted in deactivation of M1 microglia, as shown by the time-dependent inhibition of CD80 expression (Figure 3D). Furthermore, Gal1-treated M1 microglia had considerably diminished colocalization of CD45 with EEA1 (an early endosomal marker), as shown by confocal microscopy, compared to LPS-stimulated microglia treated with vehicle control (Figure 3E), consistent with decreased internalization of CD45. Functionally, binding of Gal1 to CD45 resulted in a time-dependent increase in phosphatase activity (Figure 3F). This effect was eliminated in the presence of a CD45-specific phosphatase inhibitor (Figure 3F), indicating that increased phosphatase activity was completely attributable to CD45. To dissect the contribution of N- and O-glycans to this effect, we transfected BV-2 microglial cells with short interfering RNA (siRNA) for C2GnT1 and GnT5, two critical glycosyltransferases required for biosynthesis of Gal1 ligands (Figure S4). Inhibition of core 2

relative median fluorescence (rMFI) (median fluorescence intensity of specific marker signal–median fluorescence intensity of unspecific signal) are shown. Bar diagrams display the relative MFI and percentage of positive cells as fold change relative to IFN-γ-treated microglia.
(D–H) Effect of Gal1 on the expression of specific activation markers of IFN-γ- or IL-4-stimulated microglia as determined by quantitative RT-PCR for iNOS (D and G) and arginase (H) mRNA or by bead-based Luminex assay for TNF (E) and CCL2 (F).
(I–M) Immunoblot blot (I) and densitometric analysis (J–M) of phospho-p38MAPK, phospho-ERK1/2, phospho-CREB, and phospho-IκB-α in neonatal microglia obtained from *Lgals1*$^{-/-}$ or WT mice, pretreated or not with Gal1 (5 μg/ml), and stimulated with LPS.
Data are representative (B and C, upper panel; I) or are the mean ± SEM (A–H and J–M) of three independent experiments. *$p < 0.05$; **$p < 0.01$; ***$p < 0.005$ versus control. AU, arbitrary units.
See also Figures S2 and S3.

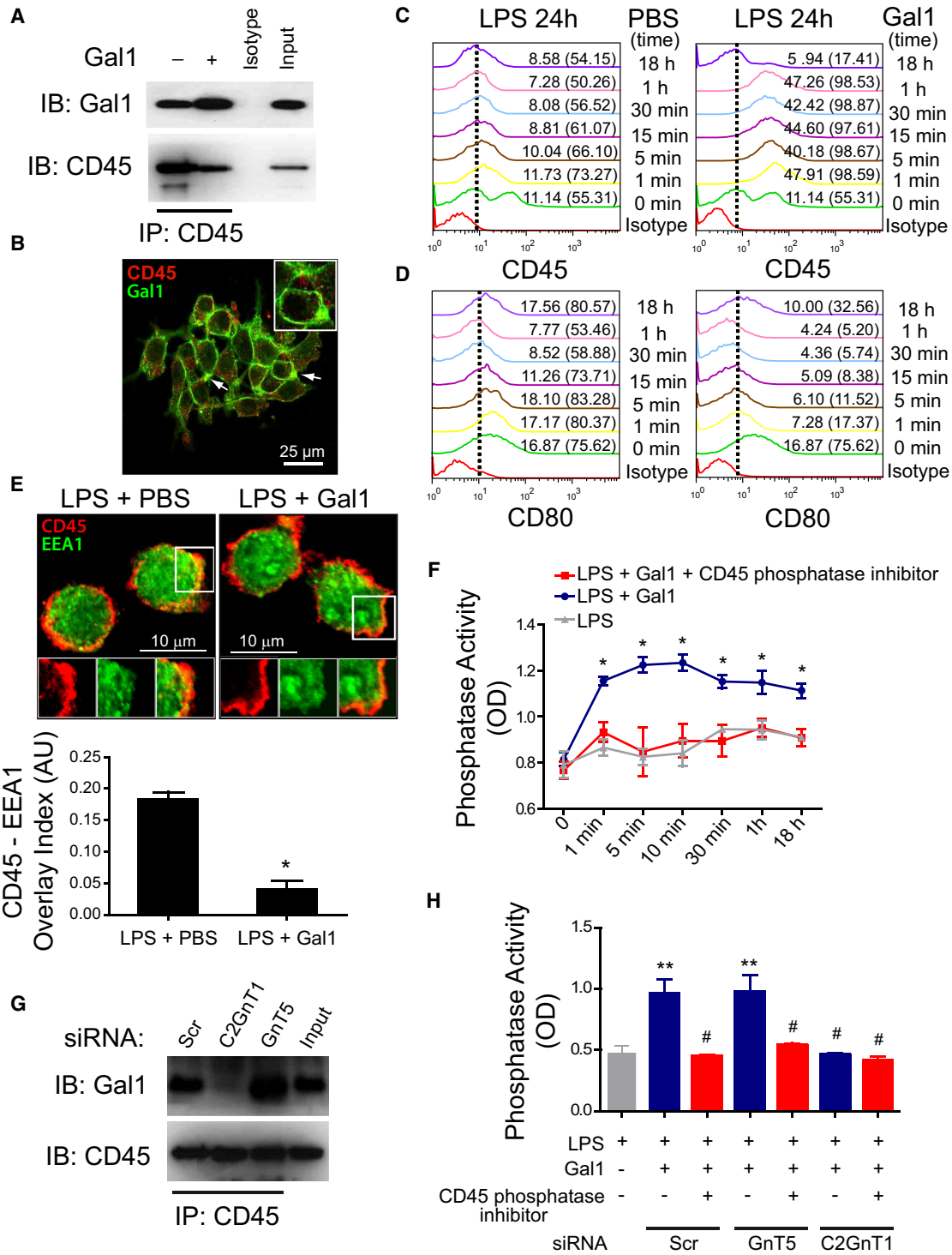

Figure 3. Gal1-Glycan Interactions Promote Retention of CD45 on the Surface of Microglial Cells and Augment its Phosphatase Activity

(A) Coimmunoprecipitation followed by immunoblotting of Gal1 and CD45 expression in lysates from microglial cells incubated with LPS (10 ng/ml) for 18 hr and further stimulated or not with recombinant Gal1. Input, whole cell lysate; IB, immunoblot; IP, immunoprecipitation.

(B) Confocal microscopy of CD45 and Gal1 colocalization in BV-2 microglial cells incubated with LPS for 18 hr and further exposed to FITC-conjugated Gal1. The scale bar represents 25 μm. The inset scale bar represents 10 μm.

(C and D) Flow-cytometry analysis of CD45 and CD80 expression in unpermeabilized BV-2 microglial cells incubated with LPS for 18 hr and then stimulated with PBS or Gal1 for the indicated time periods. Nonspecific binding determined with isotype-matched control antibodies is shown for treatment at t = 1 min. Numbers outside parentheses show the percentage of positive cells. Numbers in parentheses represent the rMFI (median fluorescence intensity of specific marker signal–median fluorescence intensity of unspecific signal) for each time analyzed.

O-glycan elongation through siRNA-mediated silencing of C2GnT1 almost completely eliminated CD45-Gal1 interactions (Figure 3G) and Gal1-induced CD45 phosphatase activity (Figure 3H), whereas interruption of complex-type N-glycan branching through siRNA-mediated GnT5 silencing had no effect (Figures 3G and 3H). Thus, O-glycan-dependent binding of Gal1 to CD45 promotes retention of this glycoprotein on the surface of microglial cells and augments its phosphatase activity.

Lack of Endogenous Gal1 Enhances Classical Microglial Activation and Promotes Axonal Damage In Vivo

Activated microglia may contribute to CNS pathology or repair, depending on the prevalent microenvironment and their mode of activation. Whereas classically activated M1 microglia are involved in inflammation-mediated neurotoxicity, alternatively activated M2 microglia have neuroprotective functions (Kigerl et al., 2009). To investigate the role of Gal1 in microglial activation in vivo, we induced EAE in *Lgals1*$^{-/-}$ and WT mice. Iba^{+}MHC II^{+} microglia were considerably more abundant in *Lgals1*$^{-/-}$ mice compared to WT EAE mice (Figure 4A), whereas healthy control mice had no Iba1^{+}MHC II^{+} cells in the CNS (data not shown). Furthermore, *Lgals1*$^{-/-}$ mice had decreased immunoreactivity against the neuronal and axonal marker β-III-tubulin (Tuj1) (Figure 4B), GAP43 (a marker for axonal growth cones) (Figure 4C), and myelin basic protein (MBP; a marker of myelination) (Figure 4D). In addition, *Lgals1*$^{-/-}$ mice showed increased GFAP^{+} astrocytes during ongoing EAE (Figure 4E). Thus, targeted deletion of endogenous Gal1 significantly increases axonal loss and decreases axonal outgrowth during autoimmune neuroinflammation.

Gal1 Controls Microglia-Mediated Neurotoxicity

To gain insight into the functional consequences of Gal1-induced microglial deactivation, we used an in vitro model of microglia-mediated neurotoxicity (Lehnardt et al., 2003). Neurons were cocultured with resting microglia, or microglia preactivated by LPS in the absence or presence of recombinant Gal1 or Gal1 alone. Because neurotoxicity is closely associated with a collapse of cytoskeleton proteins (Takeuchi et al., 2005), we measured the intensity of immunoreactivity against microtubule-associated protein 2 (Map2), the density of Map2^{+} cells, and the percentage of beaded axons. Coculture with LPS-activated microglia resulted in decreased neuronal density, with lower Map2 immunoreactivity and a higher percentage of beaded axons (Figures 5A–5D). Interestingly, coculture with microglia preactivated with LPS and Gal1 showed significantly better preservation of neurons (Figures 5A–5D). Moreover, Gal1-treated resting microglia behaved like resting microglia (Figures 5A–5D). Similar results were observed with the microglial cell line BV-2 (Figures S5A–S5D). Furthermore, direct addition of Gal1 to neuronal cultures had no major effect as the density of surviving neurons, collapse of the cytoskeleton protein Map2, and axonal beading were not significantly altered (Figures S5E–5H). Thus, Gal1 provides neuroprotection through deactivation of M1 microglia.

Astrocytes Control Microglial Activation via Gal1

As astrocytes express substantial amounts of Gal1 during both the acute and chronic phases of EAE (Figure 1D), we investigated whether Gal1 contributes to astrocyte-mediated control of microglial activation. We stimulated *Lgals1*$^{-/-}$ or WT neonatal astrocytes with PBS or TGF-β1. Exposure to TGF-β1 led to higher expression and secretion of Gal1 by astrocytes compared to astrocytes cultured with vehicle control (Figure 1G). The resulting astrocyte-conditioned medium was transferred to cultures of IFN-γ-activated neonatal M1 microglia. There were no significant differences in MHC II expression in microglia incubated with conditioned media from WT or *Lgals1*$^{-/-}$ astrocytes exposed to vehicle control. However, M1 microglia that had been exposed to conditioned media from TGF-β1-treated WT astrocytes showed decreased activation, whereas transfer of conditioned medium from TGF-β1-treated *Lgals1*$^{-/-}$ astrocytes resulted in increased microglial activation (Figure 6A).

To test this hypothesis in vivo, we injected neonatal astrocytes (5×10^{5} per mouse) from *Lgals1*$^{-/-}$ or WT mice into the right lateral ventricle of *Lgals1*$^{-/-}$ mice with EAE when they reached a clinical score of 1 (Figures 6B and S6). Adoptive transfer of Gal1-sufficient astrocytes to EAE-recipient *Lgals1*$^{-/-}$ mice successfully limited the severity of the disease, whereas injection of *Lgals1*$^{-/-}$ astrocytes failed to rescue the disease phenotype (Figure 6C). However, WT astrocytes could not exert this suppressive effect when adoptively transferred to *Lgals1*$^{-/-}$ recipient mice which had been previously injected (days 7 and 9) with clodronate-containing lyposomes for depletion of the microglial and macrophage compartments (Figure 6C). These data identify a CNS regulatory circuit by which astrocytes contribute to the resolution of autoimmune neuroinflammation via Gal1-dependent control of microglial activation.

(E) Confocal microscopy of CD45 internalization in LPS-stimulated microglial cells treated with Gal1 or vehicle control for 30 min. Cells were fixed, permeabilized, and probed with monoclonal antibodies against CD45 and EEA1. Upper panel, representative images of EEA1 (green)- and CD45 (red)-stained microglial cells. The scale bar represents 25 μm. The inset scale bar represents 10 μm. Lower panel, CD45/EEA1 overlay normalized to total EEA1 staining determined by MBF-ImageJ Colocalization Analysis by defining a box of set dimensions and scoring the incidence of superposition in six randomly selected areas.

(F) CD45-specific phosphatase activity in microglia treated with LPS and further exposed to Gal1 in the absence or presence of a CD45-specific phosphatase inhibitor for the indicated time periods.

(G) Coimmunoprecipitation followed by immunoblotting of Gal1 and CD45 expression in lysates from microglial cells transfected with C2GnT1, GnT5, or scrambled (Scr) siRNA, stimulated with LPS (10 ng/ml) and further treated with Gal1. Input, whole-cell lysate. Data are representative of two independent experiments.

(H) CD45-specific phosphatase activity in microglial cells transfected with GnT5, C2GnT1, or Scr siRNA, treated with LPS and further exposed to Gal1 for 30 min in the absence or presence of a CD45-specific phosphatase inhibitor. Similar results were observed by preincubating BV-2 microglial cells with Gal1 before exposure to LPS, as in Figure 2.

Data are representative (A–E, G) or are the mean ± SEM (E lower panel, F, H) of three independent experiments. *$p < 0.05$ versus LPS; **$p < 0.01$ versus LPS; $^{\#}p < 0.05$ versus LPS plus Gal1. OD, optical density.

See also Figure S4.

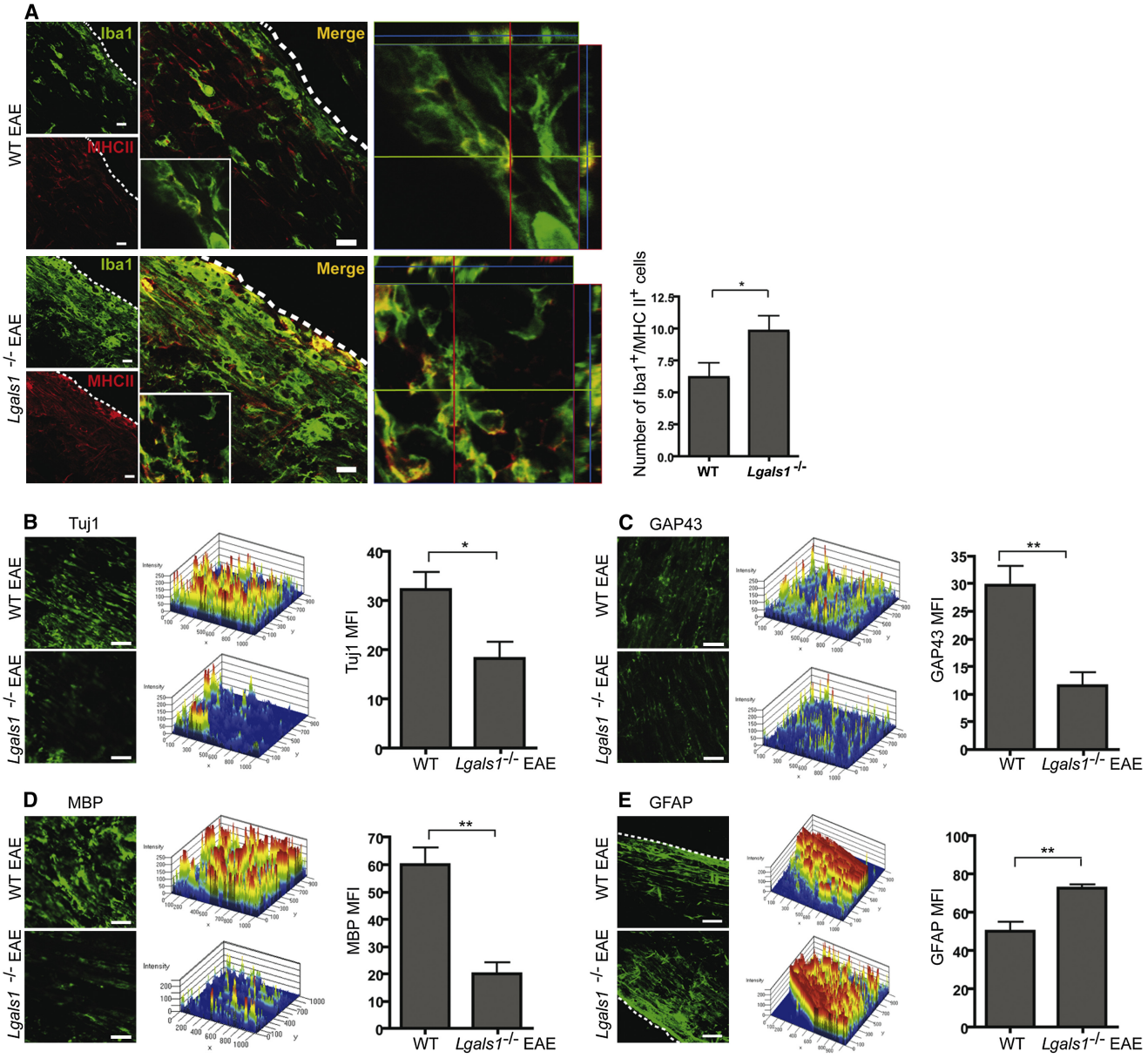

Figure 4. Endogenous Gal1 Controls Classical Microglial Activation In Vivo and Limits EAE Neuropathology

(A–E) Confocal microscopy of spinal cord white matter of WT and *Lgals1*$^{-/-}$ mice 35 days after immunization with MOG_{35-55}. Data are representative (images) or are the mean (bars) ± SEM of three independent experiments. *$p < 0.05$; **$p < 0.01$.

(A) Left, spinal cord sections were stained for Iba1 (green) and MHC II (red). Insert shows low-magnification micrograph of representative cells. Middle, 3D reconstruction ortho-view of low-magnification micrograph. Right, quantification of MHC II, Iba1 double positive microglial cells (n = 20).

(B) Left, spinal cord sections were stained for Tuj1 (green). Middle, 2.5D-intensity analysis of Tuj1 staining. Right, MFI of immunoreactivity against Tuj1.

(C) Left, spinal cord sections were stained for GAP43 (green). Middle, 2.5D-intensity analysis of GAP43 staining. Right, MFI of immunoreactivity against GAP43.

(D) Left, spinal cord sections were stained for MBP (green). Middle, 2.5D-intensity analysis of MBP staining. Right, MFI of immunoreactivity against MBP.

(E) Left, spinal cord sections were stained for GFAP (green). Middle, 2.5D-intensity analysis of GFAP staining. Right, MFI of immunoreactivity against GFAP. Scale bars represent 20 μm.

Gal1 Therapy Decreases Microglial Activation and Prevents Neurodegeneration and Demyelination

To investigate whether Gal1 therapy influences EAE neuropathology, we initiated treatment around the onset of clinical disease (day 9 to 13 postimmunization), after inflammatory cells had already entered the CNS. Administration of Gal1 significantly attenuated EAE severity (Figures 7A and 7B) and decreased microglial activation in the spinal cord (Figure 7C). Accordingly, axonal damage, neuronal degeneration, and demyelination were substantially reduced in Gal1-treated mice, as reflected by increased staining of Tuj1, GAP43, and MBP (Figures 7D–7F). Furthermore, Gal1 treatment also reduced GFAP

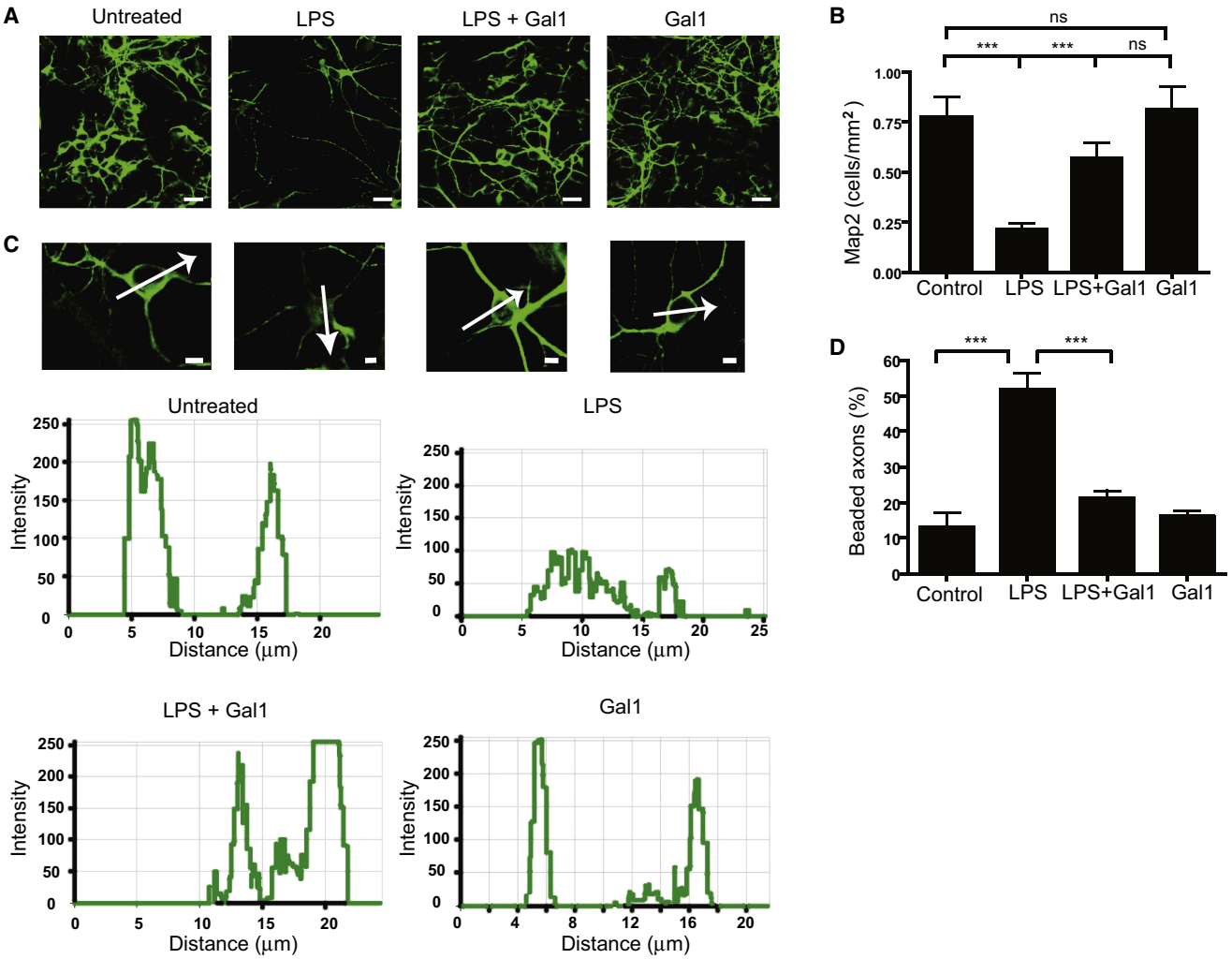

Figure 5. Gal1 Negatively Regulates Microglia-Induced Neurotoxicity

(A–D) Twenty-four-hour coculture of pretreated microglia (untreated MG, LPS-treated MG, LPS plus Gal1-treated MG, and Gal1-treated MG) with high-density cortical-neuronal cultures.

(A) Representative fluorescence photomicrographs of $Map2^+$ (green) neurons. The scale bar represents 50 μm.

(B) Density of $Map2^+$ cell bodies per mm^2 (n = 10).

(C) High-magnification photomicrographs of single $Map2^+$ neurons and pixel-intensity analysis (below). The scale bar represents 5 μm.

(D) Percentage of beaded axons per total axons (n = 10).

Data are representative (A and C) or are the mean ± SEM (B and D) of three independent experiments. ***$p < 0.005$.

See also Figure S5.

immunoreactivity (Figure 7G). Of note, administration of recombinant Gal1 to WT mice or transfer of Gal1-expressing astrocytes in *Lgals1*$^{-/-}$ EAE-recipient mice also limited the viability of CNS mononuclear cells, even in the absence of microglia (Figure S7), suggesting multiple cellular targets of Gal1 effects.

To definitively implicate microglia in the beneficial effects of Gal1 on EAE, we stimulated neonatal microglia with LPS, Gal1, or LPS plus Gal1 for 24 hr and injected them (5×10^5 per mouse) into the right lateral ventricle of *Lgals1*$^{-/-}$ mice on day 9 postimmunization (Figure 7H). Transfer of LPS-treated microglia resulted in worsening of the clinical score compared to untreated microglia (Figure 7I). Remarkably, transfer of microglia treated with both LPS and Gal1 significantly ameliorated clinical disease compared to LPS-treated microglia. Furthermore, transfer of Gal1-treated resting microglia resulted in an even lower clinical disease course compared to untreated resting microglia (Figure 7I), suggesting that Gal1 treatment may prevent the in vivo activation of microglia after intracranial transfer.

DISCUSSION

In this study we identified a CNS regulatory circuit, mediated by Gal1-glycan interactions, that contributes to neuroprotection by deactivating classically activated microglia and inducing an alternative M2 microglial phenotype. Endogenous Gal1 was upregulated in preclinical EAE, peaked during acute EAE, and

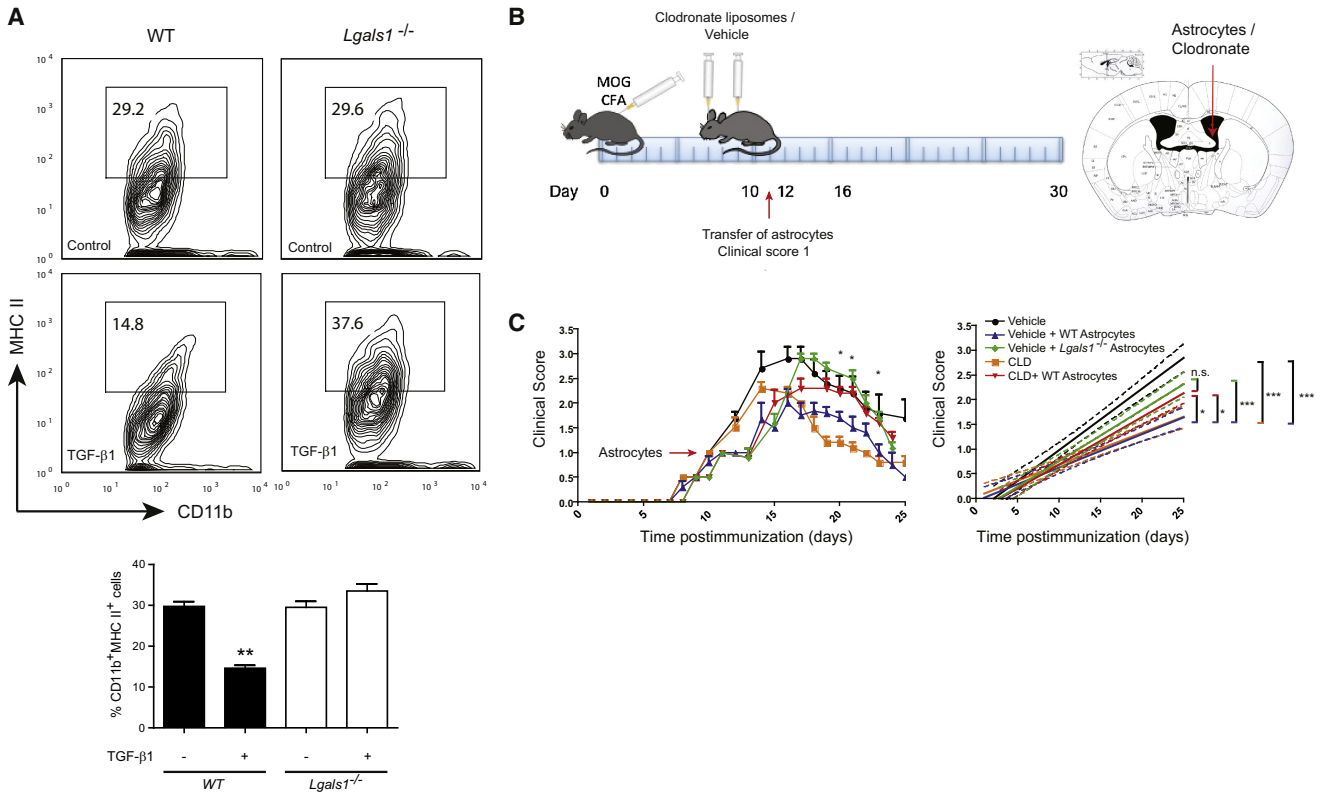

Figure 6. Astrocytes Control Microglial Activation and Limit EAE Severity via Gal1

(A) Flow cytometry of MHC II in cultured CD11b$^+$ microglia. Microglia were exposed to conditioned media from control or TGF-β1-stimulated WT or *Lgals1*$^{-/-}$ astrocytes. Percentage of CD11b$^+$MHC II$^+$ cells.

(B and C) *Lgals1*$^{-/-}$ mice were immunized with 200 μg MOG_{35-55} and injected with PBS (vehicle) or clodronate-containing liposomes (CLD) into the right lateral ventricle (day 7 and 9 postimmunization). When reaching a clinical score of 1, mice were divided into two groups and received either WT or *Lgals1*$^{-/-}$ (knockout) astrocytes into the same injection site.

(B) Diagram illustrating the experimental timeline (left) and injection site (right).

(C) Clinical score (left) and linear-regression curves of disease (right) for each group (dashed lines, 95% confidence intervals).

Data are representative (A, upper panel) or are the mean ± SEM (A, lower panel; C) of three independent experiments. *p < 0.05; **p < 0.01; ***p < 0.005.

See also Figure S6.

remained elevated, though to a lesser extent, during the chronic phase of the disease. Whereas during preclinical and acute EAE, Gal1 was expressed by astrocytes and a subpopulation of CD4$^+$ T cells and CD11b$^+$ cells, during chronic EAE, its expression was mainly restricted to astrocytes. Furthermore, anti-inflammatory stimuli, including Gal1 itself, increased Gal1 synthesis by astrocytes, an effect which was critical in limiting microglial activation. Interestingly, we observed increased GFAP immunoreactivity in the inflamed CNS of *Lgals1*$^{-/-}$ mice and decreased GFAP reactivity following Gal1 treatment. In this regard, previous studies indicated that Gal1 promotes astrocyte maturation and inhibits astrocyte proliferation in vitro (Sasaki et al., 2004). Thus, it is probable that, in addition to microglial cells, astrocytes may also respond to Gal1 and contribute to disease modulation by promoting a neuroprotective microenvironment. Moreover, our data show that CNS-infiltrating FoxP3$^+$ Treg cells express more Gal1 than FoxP3$^-$ effector T cells during preclinical disease, in accordance with the suggested role of Gal1 as a mediator of the immunosuppressive function of Treg cells (Garín et al., 2007).

Classically activated microglia are associated with neurodegeneration, whereas alternatively activated microglia have been shown to be anti-inflammatory and neuroprotective (Kigerl et al., 2009). We found that Gal1 displayed a significantly higher affinity to M1-type microglia, which respond to this lectin by downregulating activation markers, proinflammatory cytokines, and iNOS expression and by upregulating markers that are otherwise only seen in M2-type microglia, such as arginase. In the absence of endogenous Gal1, classical microglial activation is favored, concurrent with an increase in demyelination and axonal loss and a reduction in endogenous synaptic repair.

Within CNS inflamed tissues, Iba1$^+$ cells may be represented either by microglia or by peripheral macrophages. Gal1 is known to suppress macrophage activation in the periphery (Barrionuevo et al., 2007); thus, it is probable that both microglia and macrophages in the CNS will respond to Gal1 with a decrease in classical activation. In this regard, it has been demonstrated that type II monocytes are critical for the resolution of brain inflammation (Weber et al., 2007), suggesting that Gal1 may contribute to this immunoregulatory effect. Likewise, other

members of the galectin family have also been associated with the control of CNS microglia. This is the case of Gal3, which is upregulated in microglia in response to ischemic brain lesions and favors myelin phagocytosis (Walther et al., 2000; Rotshenker et al., 2008), and Gal9, which signals through Tim-3 on $CD11b^+$ CNS cells to stimulate innate immunity (Anderson et al., 2007). Furthermore, Gal3 and Gal4 are highly expressed in oligodendrocytes, favor remyelination, and contribute to amplifying CNS inflammatory responses (Pasquini et al., 2011; Wei et al., 2007; Stancic et al., 2012; Jiang et al., 2009; Jeon et al., 2010). Strikingly, cell-surface binding of Gal1, as well as the glycoprofile of classically activated microglia, recapitulates the pattern observed on Th1 and Th17 cells and in mature DCs, whereas the repertoire of cell-surface glycans observed on alternatively activated microglia is much more similar to that displayed by Th2 cells and immature DCs (Toscano et al., 2007; Bax et al., 2007).

Emerging evidence indicates that multivalent lectin-glycan interactions function by trapping glycoprotein receptors at the cell surface and preventing their endocytosis. This effect enhances receptor responsiveness to extracellular inputs and prolongs intracellular signaling (Rabinovich and Croci, 2012). Illustrating this concept, interactions between Gal3 and GnT5-modified N-glycans on TGF-βR or CTLA-4 (Partridge et al., 2004; Lau et al., 2007) and binding of Gal9 to complex N-glycans on the glucose transporter GLUT-2 (Ohtsubo et al., 2005) act by prolonging the cell-surface half life of these receptors. Here we found that Gal1 bound to core 2 O-glycans decorating CD45 on microglial cells, leading to retention of this glycoprotein on the plasma membrane and augmenting its phosphatase activity. In line with these findings, recent studies demonstrated that CD45 negatively regulates M1 microglia activation, leading to the promotion of an M2 phenotype (Salemi et al., 2011). However, CD45 phosphatase activity is also a target of the immunoregulatory activity of Gal1 and the macrophage galactose lectin (MGL) within the T cell compartment (Earl et al., 2010, van Vliet et al., 2006). Interestingly, O-glycosylation may dampen immune responses not only by preventing receptor internalization, but also by blocking receptor-ligand interactions. Binding of Gal3 to core 2 O-glycans decorating tumor-associated MHC I-related chain A (MICA) reduces the affinity of MICA for the NKG2D receptor and impairs natural killer cell activation (Tsuboi et al., 2011). Thus, lectin-glycan interactions can adjust thresholds of cellular activation and survival through modulation of endocytosis, trafficking, and signaling of canonical receptors.

Our results demonstrate that Gal1 indirectly decreased neuronal loss through mechanisms involving p38MAPK-, CREB-, and NF-κB-dependent signaling pathways, which are activated upstream of the neurotoxic molecules TNF and NO in the microglia. Notably, in our experiments, we found no direct effect of Gal1 on cultured neurons, different from a previous report on neurons derived from engineered mouse embryonic stem cells (Plachta et al., 2007). The divergence with our findings may be related to the source and biochemical properties of Gal1 used, including the prevalence of monomeric versus dimeric or oxidized versus reduced forms of the protein. The degeneration of peripheral neuronal processes in *Lgals1*$^{-/-}$ mice may be due to the loss of endogenous neuron-derived Gal1 or to differences between the peripheral nervous system and the CNS.

Several circuits, mediated by astrocytes and microglia, were reported to modulate CNS inflammation, including those involving Act1, a critical component of IL-17 signaling (Kang et al., 2010). We found that IL-17 did not considerably alter Gal1 expression in microglia or astrocytes. However, given the relevance of the IL-17-IL-17R axis in CNS pathology (Kang et al., 2010; Kawanokuchi et al., 2008), future studies are warranted to examine the crosstalk between Gal1 and IL-17 signaling in inflammation-induced neurodegeneration.

In summary, we identified a CNS regulatory circuit by which astrocytes negatively regulate microglial activation and temper disease severity through Gal1-dependent mechanisms. Our data confirm a protective role of Gal1 in autoimmune inflammation (Offner et al., 1990; Toscano et al., 2007) and demonstrate that EAE amelioration and the underlying mechanisms of neuroprotection are mediated by inactivation of M1 microglia, suggesting that the establishment of Gal1-glycan interactions among different glial cells may provide an endogenous mechanism to limit neuropathology. Thus, targeting the Gal1-glycan axis may represent a new therapeutic approach for diseases involving inflammation-associated neurodegenedration, such as MS as well as Alzheimer's and Parkinson's disease.

EXPERIMENTAL PROCEDURES

Mice and EAE Induction

Female C57BL/6 mice were purchased from the Jackson Laboratory (Bar Harbor, ME, USA). *Lgals1*$^{-/-}$ mice (C57BL/6) were provided by F. Poirier (Institute Jacques Monod, Paris). The encephalitogenic MOG_{35-55} peptide (M-E-V-G-W-Y-R-S-P-F-S-R-V-V-H-L-Y-R-N-G-K) was synthesized by the Biopolymer Laboratory (University of California, Los Angeles) and purified to > 99% via high-pressure liquid chromatography. *Lgals1*$^{-/-}$ and WT mice were immunized subcutaneously in two sites (left and right flanks) with 150 μg of MOG_{35-55} peptide that was emulsified in complete Freund's adjuvant (CFA; Sigma-Aldrich, St. Louis) containing 200 μg *Mycobacterium tuberculosis* (Difco, Detroit). Mice received 200 ng pertussis toxin (PT; List Biological, Campbell, CA, USA) in 0.2 ml PBS by intraperitoneal injections at the time of immunization and 48 hr later. Control mice were immunized with CFA followed by PT. Mice were scored daily as follows: 0, no disease; 1, loss of tail tone; 1.5, poor righting ability; 2, hind-limb weakness; 3, hind-limb paralysis; 4, quadreparesis; and 5, moribund. All animals were housed in pathogen-free facilities at the Institute of Biology and Experimental Medicine (Buenos Aires) or at the New Research Building, Harvard Medical School (Boston) according to National Institutes of Health (NIH) guidelines. All experiments were performed with the approval of the Harvard Medical Area Standing Committee on Animals and the institutional review board of the Institute of Biology and Experimental Medicine.

Preparation of Recombinant Gal1

Purification of recombinant Gal1 was accomplished as outlined previously (Barrionuevo et al., 2007). Potential LPS contamination was carefully removed by Detoxi-Gel (Pierce) and tested with a Gel Clot Limulus Test (<0.5 IU/mg; Associates of Cape Cod, Falmouth, MA, USA).

Isolation and Culture of Microglia and Astrocytes

Brains from neonatal C57BL/6 WT or *Lgals1*$^{-/-}$ mice (P0–P2) were stripped of their meninges and minced in Ca^{2+}-free Hank's balanced salt solution (HBSS). Neural tissue was digested with the Neural Tissue Dissociation Kit (P) (Miltenyi Biotec). The cell suspension was cultured in microglial culture medium (Dulbecco's modified Eagle's medium with 10% fetal bovine serum), penicillin (50 U/ml), streptomycin (50 μg/ml), sodium pyruvate (1 mM) and L-glutamine (2 mM) at 37°C and 5% CO_2. Fresh medium was added to the culture every

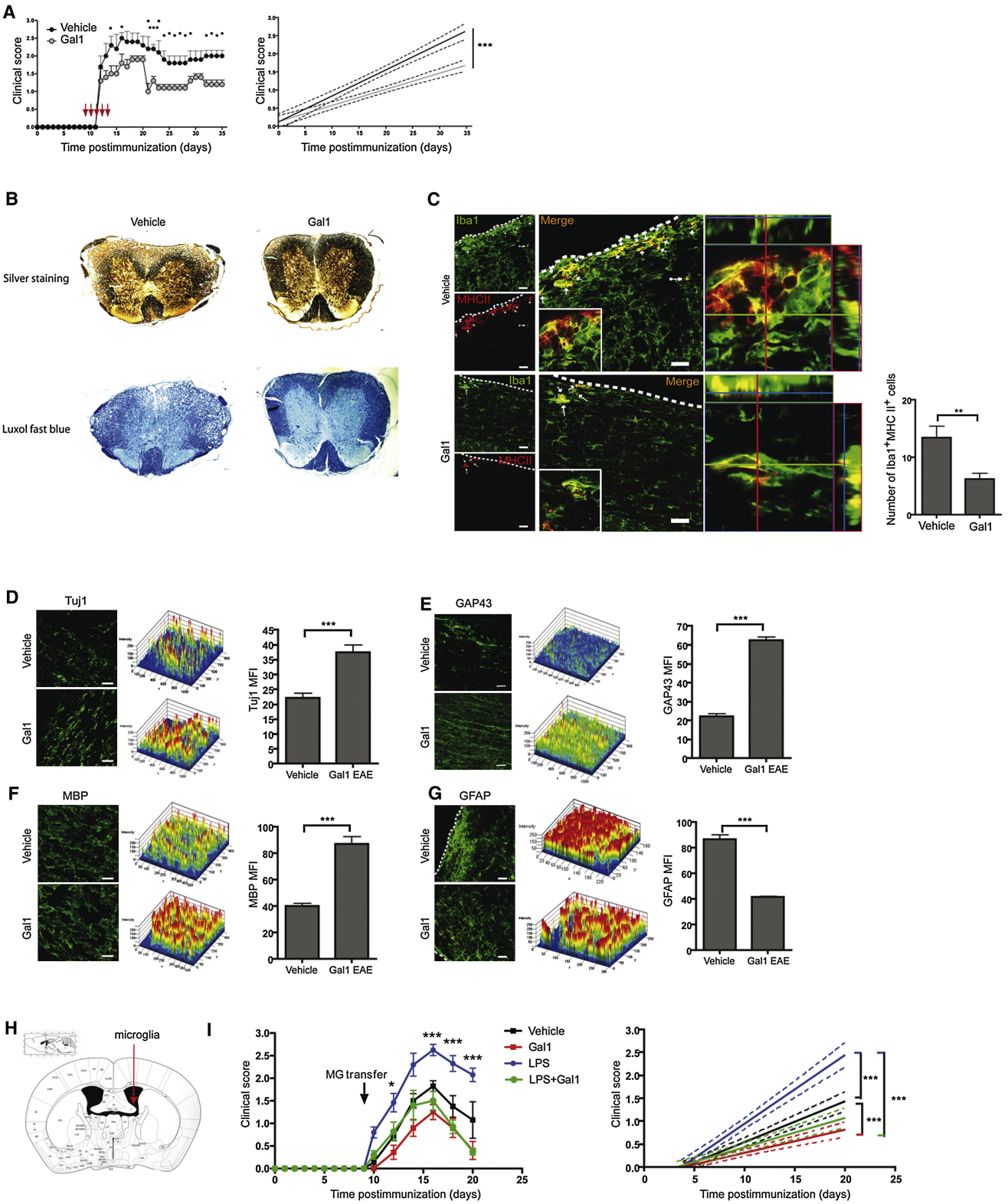

Figure 7. Gal1 Therapy Ameliorates EAE, Limits Microglia Activation, Controls Axonal Loss, and Promotes Synaptic Repair

(A) Disease score (left) of vehicle-treated and Gal1-treated (100 μg/ day) mice, immunized with 200 μg MOG_{35-55} and linear-regression curves of disease for each group (right, dashed lines, 95% confidence intervals).

(B) Bielschowsky silver (upper panel) and Luxol fast blue (lower panel) staining of spinal cord after 35 days of EAE in Gal1- or vehicle-treated mice.

(C–G) Confocal microscopy of spinal cord white matter on day 35 postimmunization in Gal1- or vehicle-treated mice.

2 days for a total period of 10–14 days. Neonatal microglial cells were shaken off the mixed brain glial cell culture after 10 to 14 days (150 rpm, 37°C, 6 hr). Microglial cells were washed and subjected to further analysis. Astrocytes for in vitro use were isolated as described (Wang et al., 2008). Astrocytes for in vivo transfer were isolated using ACSA-1 MicroBead Kit (Miltenyi Biotec). The ACSA-1 (Astrocyte Cell Surface Antigen-1) antibody is specific for the astrocyte transmembrane glycoprotein GLAST (Storck et al., 1992). Purity of astrocyte preparations was checked with a GFAP antibody (BD Biosciences). Astrocytes or microglia were stimulated with LPS (10 ng/ml), IFN-γ (10 ng/ml), IL-17 (10 ng/ml), IL-4 (10 ng/ml), IL-13 (10 ng/ml), TGF-β1 (5 ng/ml) or Gal1 (5 μg/ml) for 48 hr. Samples were stored at –80°C until subjected to further analysis. Most in vitro deactivation experiments, particularly those involving primary isolated microglia, were performed by preincubating cells with Gal1 for short periods (15 min to 2 hr) before adding LPS, whereas experiments using BV-2 microglial cells (CD45 retention, endocytosis, phosphatase activity and phenotypic markers) were conducted either by preincubating, coincubating, or adding Gal1 for different time periods after LPS treatment, yielding similar results.

Immunoblotting and Coimmunoprecipitation

Primary neonatal microglia from WT and *Lgals1*$^{-/-}$ mice were preincubated with or without recombinant Gal1 (25 μg/ml) for 15 min followed by stimulation with LPS (100 ng/ml). Cells were then washed, lysed, and subjected to immunoblot analysis with the use of antibodies against phosphorylated and unphosphorylated signaling molecules (all from Cell Signaling) as described (Ilarregui et al., 2009). For coimmunoprecipitation, 500 μg cell lysates were incubated with 2 μg anti-CD45 or isotype-control antibodies (eBioscience). The immunocomplexes were captured with Protein G PLUS-Agarose (Santa Cruz Biotechnology) and processed for immunoblotting.

Flow-Cytometry and Glycophenotypic Analysis

For assessment of Gal1 binding, recombinant Gal1 was preabsorbed with biotinylated Gal1 antibody (R&D) overnight at 4°C. Prestimulated microglial cells were incubated with increasing concentrations of preabsorbed Gal1 in the absence or presence of lactose or sucrose for 1 hr at 37°C. Cells were then incubated with allophycocyanin (APC)-conjugated streptavidin (BD Biosciences) for 15 min at 4°C. For glycophenotyping, microglial cells were stimulated with or without LPS, IFN-γ, or IL-4 for 24 hr and then stained with biotinylated SNA (20 μg/ml; Vector), PNA (20 μg/ml; Sigma-Aldrich), L-PHA (2 μg/ml; Vector), HPA (20 μg/ml; Sigma-Aldrich), or MAL II (5 μg/ml; Vector) followed by fluorescein isothiocyanate (FITC)-conjugated strepatavidin. Nonspecific binding was determined with FITC-streptavidin alone. For assessment of microglial activation, microglial cells (1 × 10^5 cells per well) were preincubated with or without recombinant Gal1 (1-10 μg/ml) for 2 hr, followed by stimulation with LPS (25–100 ng/ml; Sigma-Aldrich), IFN-γ (10–100 ng/ml; R&D) or IL-4 (10 ng/ml; BD Biosciences) for 24–48 hr. Nonspecific binding was blocked by incubation with mouse CD16/CD32 antibody (BD Biosciences) for 5 min and then surface stained with various surface markers according to the manufacturer's instructions (BD Biosciences). Cell-surface expression of CD45 and CD80 was assessed with Alexa Fluor 647-labeled CD45R (BD Bioscience) and CD80 (eBioscience) antibodies. Cells were then analyzed on a LSRII or FACSAria flow cytometer (BD Biosciences).

Cocultures of Microglial and Neuronal Cells

Neuronal cultures were prepared from E16–18 cortices. Meninges were stripped from the brain, and cortices were minced in Ca^{2+}-free HBSS. Neural tissue was digested with the Neural Tissue Dissociation Kit (P) (Miltenyi Biotec). The cell suspension was washed and plated at 5 × 10^4 cells per well on laminin (Invitrogen)-precoated glass coverslips (10 mm diameter; Electron Microscopy Sciences) and cultured in Neurobasal Medium (Sigma-Aldrich) with 2% B27 supplement (Sigma-Aldrich), penicillin (50 U/ml), streptomycin (50 μg/ml), sodium pyruvate (1 mM), and L-glutamine (2 mM) at 37°C and 5% CO_2. Fresh medium was added every 2 days for a total of 7–10 days. For examination of the direct effect of Gal1, neurons were cultured with or without recombinant Gal1 (25 μg/ml) for 48 hr. For neuro-glial cocultures, freshly isolated primary microglial or BV-2 cells were cultured in microglial culture medium, preincubated with or without recombinant Gal1 (10 μg/ml) for 15 min, and further stimulated with our without LPS (100 ng/ml) for 24 hr. Stimulated microglial cells (15 × 10^3 cells per well) were seeded with neuronal cultures and cocultured for 48 hr.

Stereotactic Transfer of Neonatal Microglia, Neonatal Astrocytes, and Clodronate-Containing Liposomes

Recipient mice (6–8 weeks old; five per group) were anesthetized with ketamine (200 mg per kg) and xylazine (10 mg per kg). Heads were secured in a sterotaxic head frame (Stoelting, Wood Dale, IL, USA). A small hole was drilled into the mouse skull, meninges were locally removed with H_2O_2, and a 10 μl Hamilton syringe with a 29G needle was inserted into the right lateral ventricle. Pretreated neonatal microglia or neonatal astrocytes (4–5 × 10^5 cells in 10 μl) or clodronate-containing liposomes (7 mg/ml; 5 μl) were injected at a flow rate of 1 μl per min at the following coordinates: anteroposterior, −0.34 mm; lateral, 1.2 mm; and dorsoventral, 2.4 mm. After completion of injection, the needle was left in place for an additional 5 min and then withdrawn at a rate of 0.5 mm per minute. The resulting wound was sutured with surgical nylon, and mice were inspected daily for postoperational care.

CD45 Phosphatase Activity

BV-2 microglial cells were preincubated with LPS (10 ng/ml) at 37°C for 18 hr, followed by stimulation with recombinant Gal1 (10 μg/ml) for different time periods, and CD45 phosphatase activity was determined essentially as described (van Vliet et al., 2006). In brief, cells were washed with ice-cold PBS and lysed in Ph lysis buffer (20 mM HEPES, pH 7.2, 2 mM EDTA, 2 mM dithiothreitol, 1% [v/v] Nonidet P-40, and 10% [v/v] glycerol containing protease inhibitors). Cellular debris and nuclear material were removed by centrifugation at 20,000 g for 15 min at 4°C. Phosphatase activity was determined by incubation of 20 μg of lysed proteins for 4 hr at 37°C with 2 mM 4-nitrophenyl phosphate (Roche) in CD45 Ph assay buffer (100 mM HEPES [pH 7.2], 2 mM EDTA, and 2 mM dithiothreitol). The resulting color change was assessed at 410 nm. Specificity was determined by the addition of a specific CD45 phosphatase inhibitor (Calbiochem).

Statistical Analysis

Prism software was used for statistical analysis. For comparison of two groups, the unpaired Student's t test was used. Significant differences were assumed at the 5% level and represented as p values ($p < 0.05$).

(C) Left, sections were stained for Iba1 (green) and MHC II (red). Insert shows low-magnification micrograph of representative cells. Middle, 3D reconstruction ortho-view of low-magnification micrograph. Right, graph represents a quantification of Iba1, MHCII double positive cells in different groups.
(D) Left, spinal cord sections were stained for Tuj1 (green). Middle, 2.5D-intensity analysis of Tuj1 staining. Right, MFI of immunoreactivity against Tuj1.
(E) Left, spinal cord sections were stained for GAP43 (green). Middle, 2.5D-intensity analysis of GAP43 staining. Right, MFI of immunoreactivity against GAP43.
(F) Left, spinal cord sections were stained for MBP (green). Middle, 2.5D-intensity analysis of MBP staining. Right, MFI of immunoreactivity against MBP.
(G) Left, spinal cord sections were stained for GFAP (green). Middle, 2.5D-intensity analysis of GFAP staining. Right, MFI of immunoreactivity against GFAP.
(H and I) Neonatal microglia were pretreated in vitro with vehicle, LPS, Gal1, or LPS plus Gal1 for 24 hr before transfer to the right lateral ventricle of *Lgals1*$^{-/-}$ EAE mice (day 9 postimmunization; n = 6 per group).
(H) Diagram illustrating the injection site.
(I) Clinical score (left) and linear-regression curves of disease for each group (right; dashed lines; 95% confidence intervals).
Scale bars represent 20 μm. Data are the mean ± SEM (A, C–G, and I) or are representative (B–G, images) of four independent experiments. *$p < 0.05$; **$p < 0.01$; ***$p < 0.005$ versus vehicle.
See also Figure S7.

SUPPLEMENTAL INFORMATION

Supplemental Information includes seven figures and Supplemental Experimental Procedures and can be found with this article online at http://dx.doi.org/10.1016/j.immuni.2012.05.023.

ACKNOWLEDGMENTS

We thank F. Poirer for *Lgals1*$^{-/-}$ mice, J. Stupirski and C. Leishman for technical assistance, and B. Waksman, B. Zhu, and M. Rubinstein for helpful discussions. This study was supported by grants from the National Multiple Sclerosis Society (RG4530 to G.A.R. and RG3945 to S.J.K.) and NIH (AI071448, AI058680 to S.J.K.), a European Recovery Program project scholarship and a doctoral fellowship of the German National Academic Foundation (to S.C.S.), the Argentinian Agency for Promotion of Science and Technology (to G.A.R.), the Mizutani Foundation for Glycoscience (to G.A.R.), the University of Buenos Aires (to G.A.R.), the Argentinian National Research Council (to G.A.R.), and Fundación SALES (to G.A.R.). We thank the Ferioli and Ostry families for donations.

Received: July 20, 2011
Revised: April 5, 2012
Accepted: May 1, 2012
Published online: August 9, 2012

REFERENCES

Anderson, A.C., Anderson, D.E., Bregoli, L., Hastings, W.D., Kassam, N., Lei, C., Chandwaskar, R., Karman, J., Su, E.W., Hirashima, M., et al. (2007). Promotion of tissue inflammation by the immune receptor Tim-3 expressed on innate immune cells. Science *318*, 1141–1143.

Barrionuevo, P., Beigier-Bompadre, M., Ilarregui, J.M., Toscano, M.A., Bianco, G.A., Isturiz, M.A., and Rabinovich, G.A. (2007). A novel function for galectin-1 at the crossroad of innate and adaptive immunity: galectin-1 regulates monocyte/macrophage physiology through a nonapoptotic ERK-dependent pathway. J. Immunol. *178*, 436–445.

Bax, M., García-Vallejo, J.J., Jang-Lee, J., North, S.J., Gilmartin, T.J., Hernández, G., Crocker, P.R., Leffler, H., Head, S.R., Haslam, S.M., et al. (2007). Dendritic cell maturation results in pronounced changes in glycan expression affecting recognition by siglecs and galectins. J. Immunol. *179*, 8216–8224.

Bitsch, A., Schuchardt, J., Bunkowski, S., Kuhlmann, T., and Brück, W. (2000). Acute axonal injury in multiple sclerosis. Correlation with demyelination and inflammation. Brain *123*, 1174–1183.

Butovsky, O., Ziv, Y., Schwartz, A., Landa, G., Talpalar, A.E., Pluchino, S., Martino, G., and Schwartz, M. (2006). Microglia activated by IL-4 or IFN-γ differentially induce neurogenesis and oligodendrogenesis from adult stem/progenitor cells. Mol. Cell. Neurosci. *31*, 149–160.

Cedeno-Laurent, F., Opperman, M., Barthel, S.R., Kuchroo, V.K., and Dimitroff, C.J. (2012). Galectin-1 triggers an immunoregulatory signature in Th cells functionally defined by IL-10 expression. J. Immunol. *188*, 3127–3137.

Correa, S.G., Sotomayor, C.E., Aoki, M.P., Maldonado, C.A., and Rabinovich, G.A. (2003). Opposite effects of galectin-1 on alternative metabolic pathways of L-arginine in resident, inflammatory, and activated macrophages. Glycobiology *13*, 119–128.

Cui, Y.Q., Zhang, L.J., Zhang, T., Luo, D.Z., Jia, Y.J., Guo, Z.X., Zhang, Q.B., Wang, X., and Wang, X.M. (2010). Inhibitory effect of fucoidan on nitric oxide production in lipopolysaccharide-activated primary microglia. Clin. Exp. Pharmacol. Physiol. *37*, 422–428.

Earl, L.A., Bi, S., and Baum, L.G. (2010). N- and O-glycans modulate galectin-1 binding, CD45 signaling, and T cell death. J. Biol. Chem. *285*, 2232–2244.

Garín, M.I., Chu, C.C., Golshayan, D., Cernuda-Morollón, E., Wait, R., and Lechler, R.I. (2007). Galectin-1: a key effector of regulation mediated by CD4+CD25+ T cells. Blood *109*, 2058–2065.

Hirabayashi, J., Hashidate, T., Arata, Y., Nishi, N., Nakamura, T., Hirashima, M., Urashima, T., Oka, T., Futai, M., Muller, W.E., et al. (2002). Oligosaccharide specificity of galectins: a search by frontal affinity chromatography. Biochim. Biophys. Acta *1572*, 232–254.

Ilarregui, J.M., Croci, D.O., Bianco, G.A., Toscano, M.A., Salatino, M., Vermeulen, M.E., Geffner, J.R., and Rabinovich, G.A. (2009). Tolerogenic signals delivered by dendritic cells to T cells through a galectin-1-driven immunoregulatory circuit involving interleukin 27 and interleukin 10. Nat. Immunol. *10*, 981–991.

Jeon, S.B., Yoon, H.J., Chang, C.Y., Koh, H.S., Jeon, S.H., and Park, E.J. (2010). Galectin-3 exerts cytokine-like regulatory actions through the JAK-STAT pathway. J. Immunol. *185*, 7037–7046.

Jiang, H.R., Al Rasebi, Z., Mensah-Brown, E., Shahin, A., Xu, D., Goodyear, C.S., Fukada, S.Y., Liu, F.T., Liew, F.Y., and Lukic, M.L. (2009). Galectin-3 deficiency reduces the severity of experimental autoimmune encephalomyelitis. J. Immunol. *182*, 1167–1173.

Kang, Z., Altuntas, C.Z., Gulen, M.F., Liu, C., Giltiay, N., Qin, H., Liu, L., Qian, W., Ransohoff, R.M., Bergmann, C., et al. (2010). Astrocyte-restricted ablation of interleukin-17-induced Act1-mediated signaling ameliorates autoimmune encephalomyelitis. Immunity *32*, 414–425.

Kawanokuchi, J., Shimizu, K., Nitta, A., Yamada, K., Mizuno, T., Takeuchi, H., and Suzumura, A. (2008). Production and functions of IL-17 in microglia. J. Neuroimmunol. *194*, 54–61.

Kigerl, K.A., Gensel, J.C., Ankeny, D.P., Alexander, J.K., Donnelly, D.J., and Popovich, P.G. (2009). Identification of two distinct macrophage subsets with divergent effects causing either neurotoxicity or regeneration in the injured mouse spinal cord. J. Neurosci. *29*, 13435–13444.

Lau, K.S., Partridge, E.A., Grigorian, A., Silvescu, C.I., Reinhold, V.N., Demetriou, M., and Dennis, J.W. (2007). Complex N-glycan number and degree of branching cooperate to regulate cell proliferation and differentiation. Cell *129*, 123–134.

Lehnardt, S., Massillon, L., Follett, P., Jensen, F.E., Ratan, R., Rosenberg, P.A., Volpe, J.J., and Vartanian, T. (2003). Activation of innate immunity in the CNS triggers neurodegeneration through a Toll-like receptor 4-dependent pathway. Proc. Natl. Acad. Sci. USA *100*, 8514–8519.

Mirzoeva, S., Koppal, T., Petrova, T.V., Lukas, T.J., Watterson, D.M., and Van Eldik, L.J. (1999). Screening in a cell-based assay for inhibitors of microglial nitric oxide production reveals calmodulin-regulated protein kinases as potential drug discovery targets. Brain Res. *844*, 126–134.

Norling, L.V., Sampaio, A.L., Cooper, D., and Perretti, M. (2008). Inhibitory control of endothelial galectin-1 on in vitro and in vivo lymphocyte trafficking. FASEB J. *22*, 682–690.

Offner, H., Celnik, B., Bringman, T.S., Casentini-Borocz, D., Nedwin, G.E., and Vandenbark, A.A. (1990). Recombinant human beta-galactoside binding lectin suppresses clinical and histological signs of experimental autoimmune encephalomyelitis. J. Neuroimmunol. *28*, 177–184.

Ohtsubo, K., Takamatsu, S., Minowa, M.T., Yoshida, A., Takeuchi, M., and Marth, J.D. (2005). Dietary and genetic control of glucose transporter 2 glycosylation promotes insulin secretion in suppressing diabetes. Cell *123*, 1307–1321.

Partridge, E.A., Le Roy, C., Di Guglielmo, G.M., Pawling, J., Cheung, P., Granovsky, M., Nabi, I.R., Wrana, J.L., and Dennis, J.W. (2004). Regulation of cytokine receptors by Golgi N-glycan processing and endocytosis. Science *306*, 120–124.

Pasquini, L.A., Millet, V., Hoyos, H.C., Giannoni, J.P., Croci, D.O., Marder, M., Liu, F.T., Rabinovich, G.A., and Pasquini, J.M. (2011). Galectin-3 drives oligodendrocyte differentiation to control myelin integrity and function. Cell Death Differ. *18*, 1746–1756.

Plachta, N., Annaheim, C., Bissière, S., Lin, S., Rüegg, M., Hoving, S., Müller, D., Poirier, F., Bibel, M., and Barde, Y.A. (2007). Identification of a lectin causing the degeneration of neuronal processes using engineered embryonic stem cells. Nat. Neurosci. *10*, 712–719.

Ponomarev, E.D., Maresz, K., Tan, Y., and Dittel, B.N. (2007). CNS-derived interleukin-4 is essential for the regulation of autoimmune inflammation and induces a state of alternative activation in microglial cells. J. Neurosci. *27*, 10714–10721.

Rabinovich, G.A., and Croci, D.O. (2012). Regulatory circuits mediated by lectin-glycan interactions in autoimmunity and cancer. Immunity *36*, 322–335.

Rasmussen, S., Wang, Y., Kivisäkk, P., Bronson, R.T., Meyer, M., Imitola, J., and Khoury, S.J. (2007). Persistent activation of microglia is associated with neuronal dysfunction of callosal projecting pathways and multiple sclerosis-like lesions in relapsing—remitting experimental autoimmune encephalomyelitis. Brain *130*, 2816–2829.

Rotshenker, S., Reichert, F., Gitik, M., Haklai, R., Elad-Sfadia, G., and Kloog, Y. (2008). Galectin-3/MAC-2, Ras and PI3K activate complement receptor-3 and scavenger receptor-AI/II mediated myelin phagocytosis in microglia. Glia *56*, 1607–1613.

Salemi, J., Obregon, D.F., Cobb, A., Reed, S., Sadic, E., Jin, J., Fernandez, F., Tan, J., and Giunta, B. (2011). Flipping the switches: CD40 and CD45 modulation of microglial activation states in HIV associated dementia (HAD). Mol. Neurodegener. *6*, 3.

Sasaki, T., Hirabayashi, J., Manya, H., Kasai, K., and Endo, T. (2004). Galectin-1 induces astrocyte differentiation, which leads to production of brain-derived neurotrophic factor. Glycobiology *14*, 357–363.

Stancic, M., Slijepcevic, D., Nomden, A., Vos, M.J., de Jonge, J.C., Sikkema, A.H., Gabius, H.J., Hoekstra, D., and Baron, W. (2012). Galectin-4, a novel neuronal regulator of myelination. Glia *60*, 919–935.

Storck, T., Schulte, S., Hofmann, K., and Stoffel, W. (1992). Structure, expression, and functional analysis of a Na(+)-dependent glutamate/aspartate transporter from rat brain. Proc. Natl. Acad. Sci. USA *89*, 10955–10959.

Stowell, S.R., Qian, Y., Karmakar, S., Koyama, N.S., Dias-Baruffi, M., Leffler, H., McEver, R.P., and Cummings, R.D. (2008). Differential roles of galectin-1 and galectin-3 in regulating leukocyte viability and cytokine secretion. J. Immunol. *180*, 3091–3102.

Takeuchi, H., Mizuno, T., Zhang, G., Wang, J., Kawanokuchi, J., Kuno, R., and Suzumura, A. (2005). Neuritic beading induced by activated microglia is an early feature of neuronal dysfunction toward neuronal death by inhibition of mitochondrial respiration and axonal transport. J. Biol. Chem. *280*, 10444–10454.

Toscano, M.A., Commodaro, A.G., Ilarregui, J.M., Bianco, G.A., Liberman, A., Serra, H.M., Hirabayashi, J., Rizzo, L.V., and Rabinovich, G.A. (2006). Galectin-1 suppresses autoimmune retinal disease by promoting concomitant Th2- and T regulatory-mediated anti-inflammatory responses. J. Immunol. *176*, 6323–6332.

Toscano, M.A., Bianco, G.A., Ilarregui, J.M., Croci, D.O., Correale, J., Hernandez, J.D., Zwirner, N.W., Poirier, F., Riley, E.M., Baum, L.G., and Rabinovich, G.A. (2007). Differential glycosylation of TH1, TH2 and TH-17 effector cells selectively regulates susceptibility to cell death. Nat. Immunol. *8*, 825–834.

Trapp, B.D., and Nave, K.-A. (2008). Multiple sclerosis: an immune or neurodegenerative disorder? Annu. Rev. Neurosci. *31*, 247–269.

Tsuboi, S., Sutoh, M., Hatakeyama, S., Hiraoka, N., Habuchi, T., Horikawa, Y., Hashimoto, Y., Yoneyama, T., Mori, K., Koie, T., et al. (2011). A novel strategy for evasion of NK cell immunity by tumours expressing core2 O-glycans. EMBO J. *30*, 3173–3185.

van der Leij, J., van den Berg, A., Harms, G., Eschbach, H., Vos, H., Zwiers, P., van Weeghel, R., Groen, H., Poppema, S., and Visser, L. (2007). Strongly enhanced IL-10 production using stable galectin-1 homodimers. Mol. Immunol. *44*, 506–513.

van Vliet, S.J., Gringhuis, S.I., Geijtenbeek, T.B., and van Kooyk, Y. (2006). Regulation of effector T cells by antigen-presenting cells via interaction of the C-type lectin MGL with CD45. Nat. Immunol. *7*, 1200–1208.

Walther, M., Kuklinski, S., Pesheva, P., Guntinas-Lichius, O., Angelov, D.N., Neiss, W.F., Asou, H., and Probstmeier, R. (2000). Galectin-3 is upregulated in microglial cells in response to ischemic brain lesions, but not to facial nerve axotomy. J. Neurosci. Res. *61*, 430–435.

Wang, Y., Imitola, J., Rasmussen, S., O'Connor, K.C., and Khoury, S.J. (2008). Paradoxical dysregulation of the neural stem cell pathway sonic hedgehog-Gli1 in autoimmune encephalomyelitis and multiple sclerosis. Ann. Neurol. *64*, 417–427.

Weber, M.S., Prod'homme, T., Youssef, S., Dunn, S.E., Rundle, C.D., Lee, L., Patarroyo, J.C., Stüve, O., Sobel, R.A., Steinman, L., and Zamvil, S.S. (2007). Type II monocytes modulate T cell-mediated central nervous system autoimmune disease. Nat. Med. *13*, 935–943.

Wei, Q., Eviatar-Ribak, T., Miskimins, W.K., and Miskimins, R. (2007). Galectin-4 is involved in p27-mediated activation of the myelin basic protein promoter. J. Neurochem. *101*, 1214–1223.

Weiner, H.L. (2009). The challenge of multiple sclerosis: how do we cure a chronic heterogeneous disease? Ann. Neurol. *65*, 239–248.

Xing, B., Xin, T., Hunter, R.L., and Bing, G. (2008). Pioglitazone inhibition of lipopolysaccharide-induced nitric oxide synthase is associated with altered activity of p38 MAP kinase and PI3K/Akt. J. Neuroinflammation *5*, 4.

Zamvil, S.S., and Steinman, L. (2003). Diverse targets for intervention during inflammatory and neurodegenerative phases of multiple sclerosis. Neuron *38*, 685–688.

Zhang, F., Qian, L., Flood, P.M., Shi, J.S., Hong, J.S., and Gao, H.M. (2010). Inhibition of IkappaB kinase-beta protects dopamine neurons against lipopolysaccharide-induced neurotoxicity. J. Pharmacol. Exp. Ther. *333*, 822–833.